Efficient waveguide lasers in femtosecond laser inscribed double-cladding waveguides of Yb:YAG ceramics

Yuechen Jia,[1] J. R. Vázquez de Aldana,[2] and Feng Chen[1,*]

[1]*School of Physics, Key Laboratory of Particle Physics and Particle Irradiation (Ministry of Education), and State Key Laboratory of Crystal Materials, Shandong University, Jinan 250100, China*
[2]*Laser Microprocessing Group, Universidad de Salamanca, Salamanca 37008, Spain*
*drfchen@sdu.edu.cn

Abstract: We report on the fabrication of depressed double-cladding waveguides in Yb:YAG ceramics by using femtosecond (fs) laser inscription. The double-cladding structures consist of tubular central structures with 30 μm diameter and concentric larger size tubular claddings with diameters of 100-200 μm. Continuous wave laser oscillations at wavelength of 1030 nm have been realized at room temperature through optical pump at 946 nm. The obtained maximum output power of the double-cladding waveguide lasers is ~80.2 mW with a slope efficiency as high as 62.9%.

OCIS codes: (230.7370) Waveguides; (140.3390) Laser materials processing; (130.3120) Integrated optics devices.

References and links

1. E. J. Murphy, *Integrated Optical Circuits and Components: Design and Applications* (Marcel Dekker, 1999).
2. C. Grivas, "Optically pumped planar waveguide lasers, Part I: Fundamentals and fabrication techniques," Prog. Quantum Electron. **35**(6), 159–239 (2011).
3. F. Chen, "Micro-and submicrometric waveguiding structures in optical crystals produced by ion beams for photonic applications," Laser Photonics Rev. **6**(5), 622–640 (2012).
4. J. Thomas, M. Heinrich, P. Zeil, V. Hilbert, K. Rademaker, R. Riedel, S. Ringleb, C. Dubs, J. P. Ruske, S. Nolte, and A. Tünnermann, "Laser direct writing: enabling monolithic and hybrid integrated solutions on the lithium niobate platform," Phys. Status Solidi A **208**(2), 276–283 (2011).
5. K. M. Davis, K. Miura, N. Sugimoto, and K. Hirao, "Writing waveguides in glass with a femtosecond laser," Opt. Lett. **21**(21), 1729–1731 (1996).
6. R. R. Gattass and E. Mazur, "Femtosecond laser micromachining in transparent materials," Nat. Photonics **2**(4), 219–225 (2008).
7. J. Burghoff, S. Nolte, and A. Tünnermann, "Origins of waveguiding in femtosecond laser-structured LiNbO$_3$," Appl. Phys., A Mater. Sci. Process. **89**(1), 127–132 (2007).
8. A. Ródenas, A. Benayas, J. R. Macdonald, J. Zhang, D. Y. Tang, D. Jaque, and A. K. Kar, "Direct laser writing of near-IR step-index buried channel waveguides in rare earth doped YAG," Opt. Lett. **36**(17), 3395–3397 (2011).
9. T. Calmano, A. G. Paschke, J. Siebenmorgen, S. T. Fredrich-Thornton, H. Yagi, K. Petermann, and G. Huber, "Characterization of an Yb:YAG ceramic waveguide laser, fabricated by the direct femtosecond-laser writing technique," Appl. Phys. B **103**(1), 1–4 (2011).
10. A. Benayas, W. F. Silva, A. Ródenas, C. Jacinto, J. Vázquez de Aldana, F. Chen, T. Tan, R. R. Thomsom, N. D. Psaila, D. T. Reid, G. A. Torchia, A. K. Kar, and D. Jaque, "Ultrafast laser writing of optical waveguides in ceramic Yb:YAG: a study of thermal and non-thermal regimes," Appl. Phys., A Mater. Sci. Process. **104**(1), 301–309 (2011).
11. A. Ródenas, G. A. Torchia, G. Lifante, E. Cantelar, J. Lamela, F. Jaque, L. Roso, and D. Jaque, "Refractive index change mechanisms in femtosecond laser written ceramic Nd:YAG waveguides: micro-spectroscopy experiments and beam propagation calculations," Appl. Phys. B **95**(1), 85–96 (2009).
12. J. Siebenmorgen, T. Calmano, K. Petermann, and G. Huber, "Highly efficient Yb:YAG channel waveguide laser written with a femtosecond-laser," Opt. Express **18**(15), 16035–16041 (2010).
13. C. Grivas, C. Corbari, G. Brambilla, and P. G. Lagoudakis, "Tunable, continuous-wave Ti:sapphire channel waveguide lasers written by femtosecond and picosecond laser pulses," Opt. Lett. **37**(22), 4630–4632 (2012).

14. Y. Tan, A. Rodenas, F. Chen, R. R. Thomson, A. K. Kar, D. Jaque, and Q. M. Lu, "70% slope efficiency from an ultrafast laser-written Nd:GdVO$_4$ channel waveguide laser," Opt. Express **18**(24), 24994–24999 (2010).
15. A. Okhrimchuk, V. Mezentsev, A. Shestakov, and I. Bennion, "Low loss depressed cladding waveguide inscribed in YAG:Nd single crystal by femtosecond laser pulses," Opt. Express **20**(4), 3832–3843 (2012).
16. D. G. Lancaster, S. Gross, H. Ebendorff-Heidepriem, K. Kuan, T. M. Monro, M. Ams, A. Fuerbach, and M. J. Withford, "Fifty percent internal slope efficiency femtosecond direct-written Tm^{3+}:ZBLAN waveguide laser," Opt. Lett. **36**(9), 1587–1589 (2011).
17. H. L. Liu, Y. C. Jia, J. R. Vázquez de Aldana, D. Jaque, and F. Chen, "Femtosecond laser inscribed cladding waveguides in Nd:YAG ceramics: fabrication, fluorescence imaging and laser performance," Opt. Express **20**(17), 18620–18629 (2012).
18. Y. Jia, F. Chen, and J. R. Vázquez de Aldana, "Efficient continuous-wave laser operation at 1064 nm in Nd:YVO$_4$ cladding waveguides produced by femtosecond laser inscription," Opt. Express **20**(15), 16801–16806 (2012).
19. H. L. Liu, Y. C. Jia, F. Chen, and J. R. Vázquez de Aldana, "Continuous wave laser operation in Nd:GGG depressed tubular cladding waveguides produced by inscription of femtosecond laser pulses," Opt. Mater. Express **3**(2), 278–283 (2013).
20. J. Lu, M. Prabhu, K. Ueda, H. Yagi, T. Yanagitani, A. Kudryashov, and A. A. Kaminskii, "Potential of ceramic YAG lasers," Laser Phys. **10**(11), 1053–1057 (2001).
21. A. Ikesue, Y. L. Aung, T. Taira, T. Kamimura, K. Yoshida, and G. L. Messing, "Progress in ceramic lasers," Annu. Rev. Mater. Res. **36**(1), 397–429 (2006).
22. A. A. Kaminskii, "Laser crystals and ceramics: recent advances," Laser Photonics Rev. **1**(2), 93–177 (2007).
23. J. Dong, A. Shirakawa, K. Ueda, H. Yagi, T. Yanagitani, and A. A. Kaminskii, "Laser-diode pumped heavy-doped Yb:YAG ceramic lasers," Opt. Lett. **32**(13), 1890–1892 (2007).
24. H. Yoshioka, S. Nakamura, T. Ogawa, and S. Wada, "Diode-pumped mode-locked Yb:YAG ceramic laser," Opt. Express **17**(11), 8919–8925 (2009).
25. A. Brenier and G. Boulon, "Overview of the best Yb^{3+}-doped laser crystals," J. Alloy. Comp. **323–324**, 210–213 (2001).
26. R. Ramponi, R. Osellame, and M. Marangoni, "Two straightforward methods for the measurement of optical losses in planar waveguides," Rev. Sci. Instrum. **73**(3), 1117–1120 (2002).
27. V. Filippov, Yu. Chamorovskii, J. Kerttula, K. Golant, M. Pessa, and O. G. Okhotnikov, "Double clad tapered fiber for high power applications," Opt. Express **16**(3), 1929–1944 (2008).

1. Introduction

As the basic components of integrated photonics and modern telecommunication systems, optical guiding structures could confine light propagation within extremely compressed volumes with dimensions of micrometric or sub-micrometric scales, in which high optical intra-cavity intensities could be obtained compared to bulks materials [1]. As a result, laser oscillations with reduced lasing thresholds may be realized in active gain waveguide configurations, possessing comparable efficiencies with respect to bulk lasers [2]. Additionally, a single photonic chip can be constructed based on waveguide platforms to achieve multiple functions [3,4]. Since the pioneering work of Davis *et al.* in 1996 [5], femtosecond (fs) laser inscription technique has been emerged to be a powerful and efficient method for the construction of three-dimensional (3D) guiding structures inside numerous transparent materials, and a wide range of photonic applications have been realized [4–19]. These guiding structures include the directly written waveguides (so-called Type I, with positive refractive index changes in the irradiated filament) [7], stress-induced waveguides (so-called Type II, typically with guiding region between the two tracks of negative index changes) [8–14] and depressed cladding waveguides (located in the core surrounded by multiple low-index tracks) [15–19].

Recently, rare-earth-doped yttrium aluminum garnet (YAG) ceramics have received wide attention [8–11], mainly owing to their intriguing advantages over the single crystalline partners, such as superior optical and thermal properties, the possibility of large-size multilayers for multipurpose laser devices, higher doping concentration as well as less fabrication-consuming [20–22]. Particularly, ytterbium doped YAG (Yb:YAG) ceramics have shown a remarkable laser performance in both continuous wave (cw) and pulsed regimes [23,24], on account of combining the outstanding fluorescence properties of Yb ions, such as long fluorescence lifetime (about 3-4 times that of Nd^{3+} ions), absence of excited state absorptions from the metastable state, minimum quantum defect between pump and laser

photons, broad emission bands, and high emission and absorption cross sections [25] with the well-known splendid properties of YAG ceramics for laser applications [22]. As of yet, only Type-II stress-induced waveguides with the dual-line design have been successfully fabricated with ultrafast pulses laser [9,10]. Compared to Type II waveguides, one of the advantages of the normal cladding waveguiding structures is that the large scale cross sections match the commercially available multimode fibers (with diameters of 100-400μm), which in principle offers an opportunity to realize efficient fiber-waveguide laser systems with low costs. However, as a drawback, the cladding waveguide lasers generally cannot exhibit single-modal beam properties as Type-II waveguides due to the large diameters of the guiding structures [17–19,26]. In this work, we propose a novel design of double-cladding configurations fabricated by fs-laser inscription technique. The geometry is similar to the well-known double-clad fibers [27]. The large diameter pump beam may be efficiently coupled into the outer clad, and the waveguide lasers will generate only through the inner core. Under optical pumping, waveguide lasers at 1030 nm wavelength with efficient continuous wave output have been realized, showing single mode behavior.
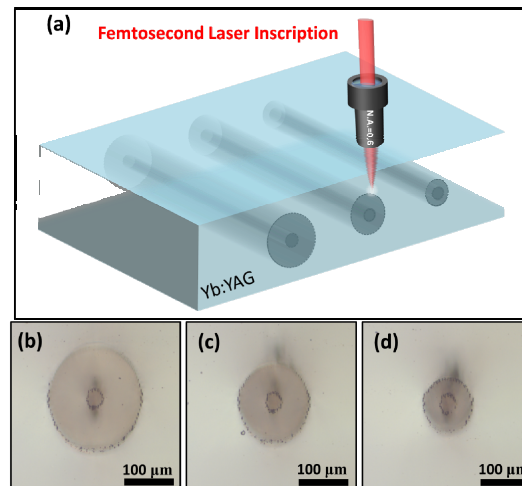
2. Experiments in details

Fig. 1. (a) Schematic of fs-laser inscription process in Yb:YAG ceramics for the double cladding waveguides, and their cross sectional microscope images, which consist of tubular central structures with 30 μm diameter, and concentric larger size tubular claddings with diameters of (b) 200, (c) 150 and (d) 100 μm, respectively.

The Yb:YAG ceramic sample (doped by 15 at. % Yb^{3+} ions, obtained from Baikowski Ltd., Japan) used in this work was cut into wafers with dimensions of $10 \times 10 \times 2$ mm^3 and optically polished. The double cladding waveguide structures were fabricated by utilizing the laser facilities at the Universidad de Salamanca, as schematized in Fig. 1(a). We used an amplified Ti:Sapphire laser system (Spitfire, Spectra Physics, USA) generating linearly-polarized 120 fs pulses at a central wavelength of 800 nm (with 1 kHz repetition rate and 1 mJ maximum pulse energy). The value of the pulse energy used to irradiate the sample was set with a calibrated neutral density filter, a half-wave plate and a linear polarizer. The sample was placed in a computer controlled motorized 3-axes stage. The beam was focused through a $40 \times$ microscope objective (N.A. = 0.65) at certain depth beneath the largest sample surface (dimensions of 10×10 mm^2), and several tests at different pulse energies and scanning velocities were performed. Optical microscopy (in transmission mode) was used to evaluate the damage tracks produced in the sample and the final irradiation parameters were fixed to 0.84 μJ of pulse energy. During the irradiation the sample was moved at a constant speed of 500 μm/s in the direction perpendicular to the laser polarization and the pulse propagation

that was carefully aligned with the 10-mm long edge of the sample, thus producing a damage track along the sample. The optimum values of velocity and pulse energy were chosen as a compromise between producing a large enough damage in the laser tracks (index contrast) and minimizing the formation of cracks in the sample. Many parallel scans (with ~3 μm separation between adjacent damage tracks) were performed at different depths of the sample (from bottom to top in order to avoid the shielding of the incident pulses by the previously written damage tracks) to inscribe the double-cladding waveguides, that consisted of a tubular central structure with 30 μm diameter, and a concentric larger size tubular claddings (100, 150 or 200 μm diameter). The cross section of the resulting structures in the Yb:YAG ceramic can be seen in Figs. 1(b)-1(d).

We performed the end-face coupling experiment with a He-Ne laser at wavelength of 632.8 nm to experimentally characterize the modal profiles of the waveguides, and the results are shown in Figs. 2(a)-2(c). From these figures, one can find that the fabricated structures exhibit very well confined modal profiles in the inner claddings, for both TE and TM polarizations. Nevertheless, all the profiles show multimode distributions, which can be well understood in terms of the large size of the structures compared to the test wavelength (632.8 nm), just like shown in previous works [17–19]. In addition, we also performed the waveguide loss measurements under 632.8 nm, taking the Fresnel reñection loss of the end facets (in our case, the value is about 0.3 dB) into account. The insertion losses of the inner claddings were estimated to be 0.8 ± 0.2 dB/cm, 1.0 ± 0.2 dB/cm and 1.3 ± 0.2 dB/cm for the double-cladding waveguides with diameters of 200, 150 and 100 μm, respectively. Differences of 0.4 dB are found between the TE and TM polarizations (the TE polarized light shows higher insertion losses than TM modes for these three waveguides). Nevertheless, this phenomenon is significantly different from the Type II Yb:YAG waveguides, which only support guidance along TM polarizations [12].
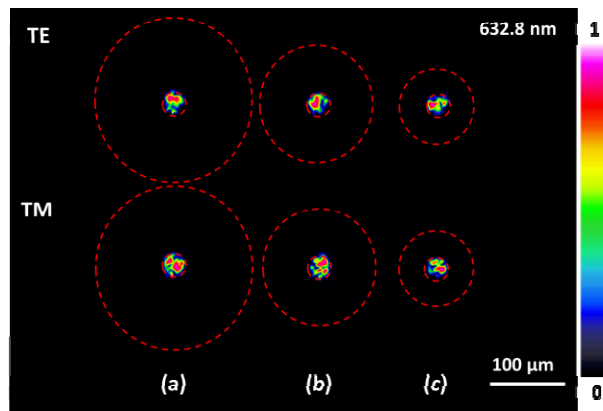

Fig. 2. Near-field modal profiles of the TE and TM guided modes (at 632.8 nm) from the double-cladding waveguides with external diameters of (a) 200, (b) 150 and (c) 100μm. The red dashed lines indicate the spatial locations of the fs-laser induced tracks. The colors bar in the right show the normalized intensity magnitude of the mode profile.

The waveguide laser experiment in this work was performed by using an end-pumped system at room temperature. We utilized a nearly linearly polarized light beam at 946 nm generated from a solid-state laser (Model MLL-H-946, CNI Optoelectronics Tech. Co. Ltd., China) as the pump source. A half-wave plate was employed to control the polarization of the pump laser beam, so that the waveguide properties in both TE and TM polarization can be investigated. A convex lens with focal length of $f = 25$ mm was used to couple the laser beam into the waveguides. The pump beam had a $1/e^2$ diameter of 1.5 mm, and was focused by the convex lens obtaining a ~20 μm diameter at the focal point. During the experiment, the distance between the convex lens and sample was carefully adjusted to obtain the optimized

coupling efficiency of the pump beam and the waveguide modal fields. In this way, the size of the pump beams at the waveguide input facet was set to ~100-200 μm of diameter. The laser cavity contains two additional dielectric mirrors. The input mirror has a high transmission of 98% at 946 nm and high reflectivity >99% at ~1030 nm, and the output mirror has a reflectivity >99% at 946 nm and a transmittance of 65% at 1030 nm. Both mirrors were adhered to the two end-facets of the waveguide sample, constructing a typical Fabry-Perot cavity. The generated laser emission was collected by a 20 × microscope objective lens (numerical aperture N.A. = 0.4), imaged by an infrared-sensitive CCD and characterized by a spectrometer and a powermeter.

3. Results and discussion

We estimated the refractive index change (Δn) of the waveguide using the equation $\Delta n = \sin^2 \Theta_m / (2n)$ [12] by measuring the N.A. of the waveguide. In this equation, $n = 1.7180$ is the substrate refractive index at 632.8 nm, and Θ_m is the maximum beam divergence of the light entering or leaving the waveguide. According to the measured $\Theta_m \approx 9°$, the effective refractive index increase can be estimated to $\Delta n \approx + 0.007$. This value is in good agreement with that of the Nd:YAG cladding waveguides [15,17].
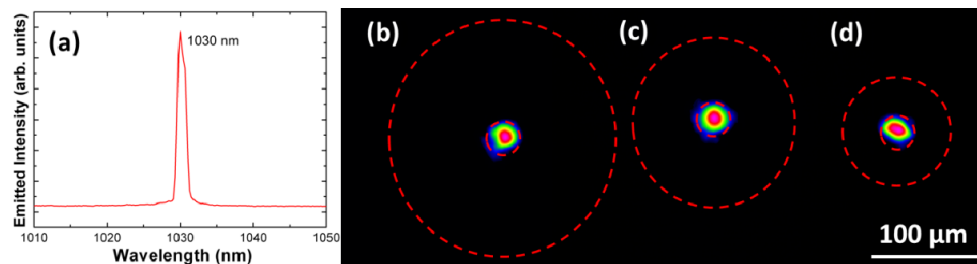

Fig. 3. (a) Spectrum of laser emissions at 1030 nm from the inner core of the 200-μm Yb:YAG ceramic double-cladding waveguide when the pumping laser was TM polarized. Laser modal profiles of the double-cladding waveguides with diameters of (b) 200, (c) 150 and (d) 100 μm at the lasing wavelength of ~1030 nm with TM polarization. The red dashed lines indicate the spatial locations of the fs-laser induced tracks.

Laser emissions were observed in all these three double-cladding waveguides, and also, laser oscillation was achieved along both of the two transverse polarizations (i.e., TE and TM), which has been found to be one of the features of cladding structures. Similar laser emission spectra and waveguide laser modal profiles were obtained from the different waveguides and the two polarizations. Figure 3(a), as a representative, exhibits the room temperature laser emission spectrum measured from the output end-facet of the inner core of 200-μm double-cladding waveguide, when the absorbed power is above the lasing threshold. The central wavelength of the laser emission is at 1030 nm with a full-width half-maximum (FWHM) of 0.9 nm. The near-field intensity distributions of the output waveguide laser generated from the three double-cladding guiding structures with TM polarization were illustrated in Figs. 3(b)-3(d), the results when the pumping laser was TE polarized were nearly the same. As we can see, similar to the data at 632.8 nm, the double-cladding waveguides supported guidance at 1030 nm from the inner core. Furthermore, the 30-μm-diameter cladding structures (i.e., the inner core of double-cladding waveguides) supported single-mode waveguide lasers, which is significantly different from the data in Fig. 2 and large scale claddings [17–19].

Figures 4(a) and 4(b) exhibit the output powers of generated TE and TM polarized lasers at 1030 nm as a function of launched pump powers at 946 nm obtained from the inner 30μm-diameter core of the three double-cladding waveguides. The launched powers (assuming the ~100% coupling efficiency of pump beam with the waveguide modal field) were measured

directly before the waveguide input facet. As one can see from the figures, for each inner core cladding waveguide, the TM polarized laser shows comparable better performance than TE polarized one, both in the achieved maximum output power ($P_{TE,100}$ = 38.4 mW, $P_{TE,150}$ = 43.6 mW and $P_{TE,200}$ = 63.5 mW against $P_{TM,100}$ = 45.8 mW, $P_{TM,150}$ = 59.1 mW and $P_{TM,200}$ = 80.2 mW). As for the slope efficiency (Φ), one can obtain that $\Phi_{TE,100}$ = 32.8%, $\Phi_{TE,150}$ = 38.3% and $\Phi_{TE,200}$ = 53.3% against $\Phi_{TM,100}$ = 38%, $\Phi_{TM,150}$ = 46.4% and $\Phi_{TM,200}$ = 62.9%. It can be partly attributed to the lower insertion loss of the TM polarization. In addition, it is obvious that as the diameters of outer claddings increases from 100 to 200 μm, the maximum output laser powers as well as the slope efficiencies increase accordingly for both TE and TM polarization (the lasing thresholds remain nearly independent on the external cladding size). Such behavior can be explained because with the same laser output volume (the 30 μm-diameter inner core cladding), the larger area of the external cladding confine more pumping light within the whole structure, resulting in comparably higher generated laser power.
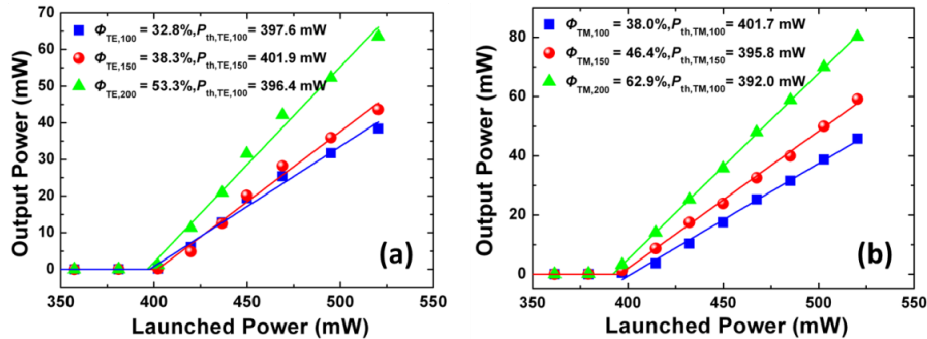

Fig. 4. Output laser power as a function of the launched pump power obtained from the inner 30 μm-diameter cores of the three double-cladding waveguides with (a) TE and (b) TM polarization, respectively. The blue square, red circular and green triangular symbols stand for the data of the double-cladding waveguides with outer diameters of 100, 150 and 200 μm, respectively. The solid lines represent the linear fit of the experimental data.

4. Summary

In conclusion, we have fabricated double-cladding waveguides in Yb:YAG ceramic, consisting of tubular central structures with 30 μm diameter and concentric larger size tubular claddings with diameters of 100-200 μm, by using fs laser inscription. Single-mode waveguide lasers at 1030 nm have been obtained for the three cladding diameters, at both TE and TM polarizations (optical pumping at 946 nm). A maximum slope efficiency as high as 62.9% and an output power of 80.2 mW was achieved under TM polarized optical pumping for the largest cladding size waveguide, which is benefited from the larger-area pump of the outermost cladding. This work paves a new way to construct a single-mode laser system with a direct fiber-waveguide configuration.